JOURNAL OF MATERIALS SCIENCE 33 (1998) 463–469

Combined effects of cerium and boron on the mechanical properties and oxidation behaviour of Ni_3Al alloy

ZEXI YUAN
Department of Materials, Wuhan Yejin University of Science and Technology, Wuhan, Hubei 430081, People's Republic of China

SHENHUA SONG, R. G. FAULKNER
Institute of Polymer Technology and Materials Engineering, Loughborough University, Loughborough, Leicestershire LE113TU, UK

ZONGSEN YU
Department of Materials Physics, University of Science and Technology Beijing, Beijing, People's Republic of China

The combined effects of cerium and boron additions on the room-temperature tensile properties and high-temperature oxidation behaviour of Ni_3Al alloys: alloy 1 doped with cerium, alloy 2 doped with boron, and alloy 3 doped with both cerium and boron. The strength, ductility and oxidation behaviour of the alloy are more effectively improved by combined cerium and boron additions than by cerium or by boron addition alone. Of the three alloys, alloy 3 exhibits comprehensively the best mechanical properties and oxidation resistance. Alloy 2 presents the better mechanical properties than alloy 1; nevertheless, alloy 1 has the better oxidation resistance than alloy 2.

1. Introduction

The intermetallic compound Ni_3Al with an $L1_2$-type ordered crystal structure, as is well known, has attractive mechanical properties and oxidation behaviour at high temperatures [1, 2], and therefore it is a potential candidate for high-temperature structural applications. However, this aluminide is brittle in the polycrystalline form. The brittleness effectively impedes its fabrication into useful structural components.

Currently there exist two mechanisms to account for the brittleness of polycrystalline Ni_3Al alloy, one of which is the intrinsic weakness of grain boundaries [3–6] and the other is the moisture-induced hydrogen embrittlement [7–9]. Segregation of moisture-induced hydrogen atoms at the crack tip or near to the tip decreases the bonding strength of grain boundaries, leading to intergranular brittle fracture.

In order to improve the ductility of the aluminide, a large amount of research has been done both experimentally and theoretically. It has been demonstrated [6, 10, 11] that minor additions of boron may enhance room-temperature tensile ductility in Ni-rich Ni_3Al alloy considerably and promote transgranular dimple fracture. Studies by Yuan *et al.* [12] have revealed that the rare-earth element, cerium, may also increase the ductility of polycrystalline Ni_3Al alloy. Segregation of the added species to grain boundaries plays a decisive role in both cases.

One of the key requirements of intermetallic compounds being considered for high-temperature applications is resistance to environmental degradation. Of the numerous modes of environmental degradation such as oxidation, corrosion by aqueous media, erosion, hydrogen embrittlement and hot corrosion, oxidation is a primary degradation mode for most intermetallic compounds that might be used for high-temperature applications. One of the reasons that Ni_3Al is considered for high-temperature applications is the formation of protective Al_2O_3 scale which has the following features: (i) high thermodynamic stability; (ii) slow growth rate (slow thickening rate); (iii) good adherence to the intermetallic substrate; (iv) easily formed and re-formed (in case of mechanical damage or oxide scale spallation).

A study on the effect of boron on oxidation behaviour of Ni_3Al [13] indicates that the aluminide with 0.52–1.37 at % B exhibits the best high-temperature oxidation resistance. Also, it has been confirmed [14] that cerium can increase oxidation resistance of a Ni–(20–25) wt % Cr high-temperature alloy. As a result, it is anticipated that combined cerium and boron additions may be able to improve more effectively the mechanical properties and oxidation behaviour of Ni_3Al alloy than cerium addition alone. In the present work, the combined effects of these two elements on the properties of Ni_3Al alloy have been examined with the aid of tensile tests, high-temperature oxidation

0022–2461

tests, scanning electron microscopy (SEM) and transmission electron microscopy (TEM).

2. Experimental procedure

The alloys used in this study were prepared by vacuum induction melting and precision casting from high-purity nickel, aluminium and cerium metals as well as a Ni–B master alloy. The size of the ingot was 6 mm × 30 mm × 120 mm. The compositions of the alloys are listed in Table I. All the original ingots were cut into ingots 3 mm × 30 mm × 120 mm in size. All the ingots were homogenized for 3 h at 1150 °C under an argon atmosphere and then fabricated into sheets 2 and 0.8 mm in thickness, respectively, by repeated rolling at room temperature with intermediate anneals at 1000 °C for 0.5 h. A reduction in thickness of 20% was applied in the first rolling and subsequently 30% after each intermediate anneal.

Sheet specimens with a gauge section of 30 mm × 4.5 mm × 0.8 mm were used for measurements of tensile properties at room temperature. The sheet specimens of the alloys were isothermally treated at 550 °C for 120 h, 750 °C for 40 h, 1000 °C for 1 h, and 1200 °C for 0.5 h in vacuum, respectively, followed by air cooling to room temperature. Tensile tests were carried out on an Autograph testing machine at a strain rate of $2.8 \times 10^{-4}\ s^{-1}$. The load–time curves were recorded on a strip chart, from which tensile data were calculated. In tensile tests, four specimens were used for each holding temperature and the arithmetic mean of data points obtained was taken as the measured result. The fracture surfaces were examined with an S-570 scanning electron microscope.

Samples 16 mm × 10 mm × 2 mm in size were mechanically polished, then cleaned in absolute alcohol and finally dried for the use of oxidation tests. Oxidation behaviour was examined by the following procedure. The samples were held for 4, 8, 16, 32, 64 and 100 h at 1000 and 1100 °C, respectively, in air, in a crucible which had been heat treated previously for some time at 1200 °C to make its mass invariable. The increase in mass of the sample after oxidation, averaged from three data points obtained, was taken as a measure of the degree of oxidation. In measuring, a balance with an accuracy of 10^{-5} g was employed and three samples for each condition.

3 mm dia. discs for TEM were cut from the samples concerned. These discs were mechanically thinned to approximately 0.1 mm thickness, followed by dual-jet electropolishing to achieve foil regions which were electron transparent. The electropolishing solution used was a solution of 5% perchloric acid and 95% methanol. Microstructural analysis was performed using a JEM-2000F analytical electron microscope in TEM mode.

Cross-sections of the oxidized samples were mechanically polished and etched in a solution consisting of 20 parts of H_2O, 20 parts of HNO_3, 10 parts of HF, 20 parts of H_3PO_4, 10 parts of acetic acid and 10 parts of HCl and then examined using optical microscopy. The structure of the oxide scale was analysed using X-ray diffraction technique.

TABLE I Chemical compositions of the alloys

Alloy	Amount (wt %)					
	C	S	Al	Ce	B	Ni
1	0.006	0.002	10.57	0.011		Balance
2	0.008	0.006	10.14		0.054	Balance
3	0.008	0.003	10.14	0.021	0.066	Balance

3. Results

3.1. Tensile properties

Room-temperature tensile properties of the alloys were determined by tensile tests of the sheet specimens 0.8 mm in thickness and shown in Table II. Table II can be summarized as follows.

For alloy 1 containing cerium, the ductility of the alloy is improved when the added quantity of cerium is relatively small. For example, the tensile elongation reaches 16%. Only for the specimens isothermally treated at 550 °C for 120 h and at 1200 °C for 0.5 h do their tensile elongation and ultimate tensile strength reach 16% and about 900 MPa, respectively. However, they are only 3% and about 500 MPa, respectively, for the specimens that were isothermally treated at 750 °C for 40 h and at 1000 °C for 1 h. The above results demonstrate that the tensile properties of

TABLE II Tensile properties of the alloys

Alloy	Holding temperature (°C)	Holding time (h)	Yield strength, $\sigma_{0.2}$ (MPa)	Ultimate tensile strength (MPa)	Elongation (%)
1	550	120	374.4	925.5	16
2			347.4	1070.9	34
3			446.9	1041.7	22
1	750	40	—	559.2	3
2			280.6	1051.6	33
3			558.6	1180.6	29
1	1000	1	—	498.1	3
2			245.8	1066.5	30
3			530.8	1017.6	26
1	1200	0.5	304.4	888.9	16
2			276.8	1075.9	35
3			406.6	937.7	24

alloy 1 strongly depends on the distribution of cerium because the distributions of cerium atoms are different at different heat treatment temperatures.

For alloy 2 containing boron and for alloy 3 containing both cerium and boron, all the samples exhibit higher yield and ultimate tensile strengths compared with alloy 1. The yield strength of alloy 3, however, is much higher than that of alloy 2. Also alloys 2 and 3 both exhibit much greater elongation than alloy 1 for all the heat-treatment conditions; nevertheless the elongation of alloy 2 is somewhat higher than that of alloy 3.

3.2. Fracture behaviour

Fracture behaviour of tensile samples, broken by tensile tests, was also studied by SEM. For alloy 1 containing cerium, SEM fractographs of the samples isothermally treated at 550 and 1200 °C are shown in Fig. 1a and b which are fractographs of the specimen treated at 550 °C, showing a large amount of ductile fracture with a small amount of intergranular fracture, and of the specimen treated at 1200 °C, showing a large amount of ductile fracture with a small amount of quasi-cleavage fracture, respectively. SEM fractographs of the samples isothermally treated at 750 and 1000 °C are shown in Fig. 2, which indicates that both specimens exhibit brittle intergranular fracture.

The fractography of boron-containing alloy 2 indicates that the samples present transgranular ductile fracture for all the heat-treatment conditions. For alloy 3 containing both cerium and boron, the samples isothermally treated at either 550 or 1200 °C exhibit a great amount of ductile fracture with a small amount

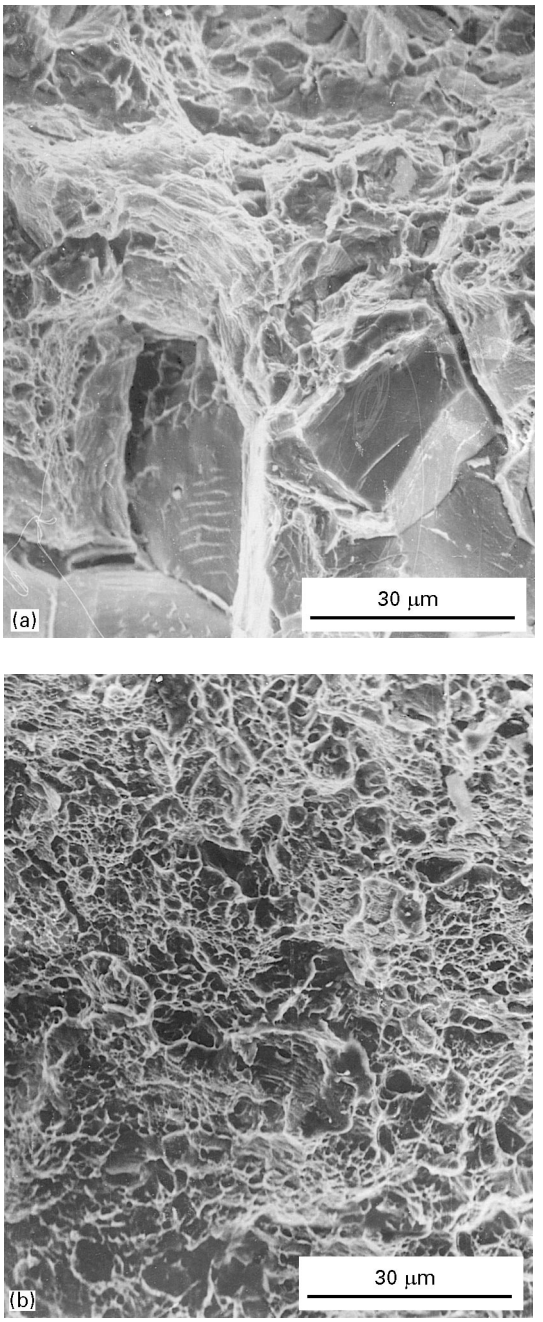

Figure 1 SEM fractographs of the alloy 1 samples isothermally treated at (a) 550 °C and (b) 1200 °C.

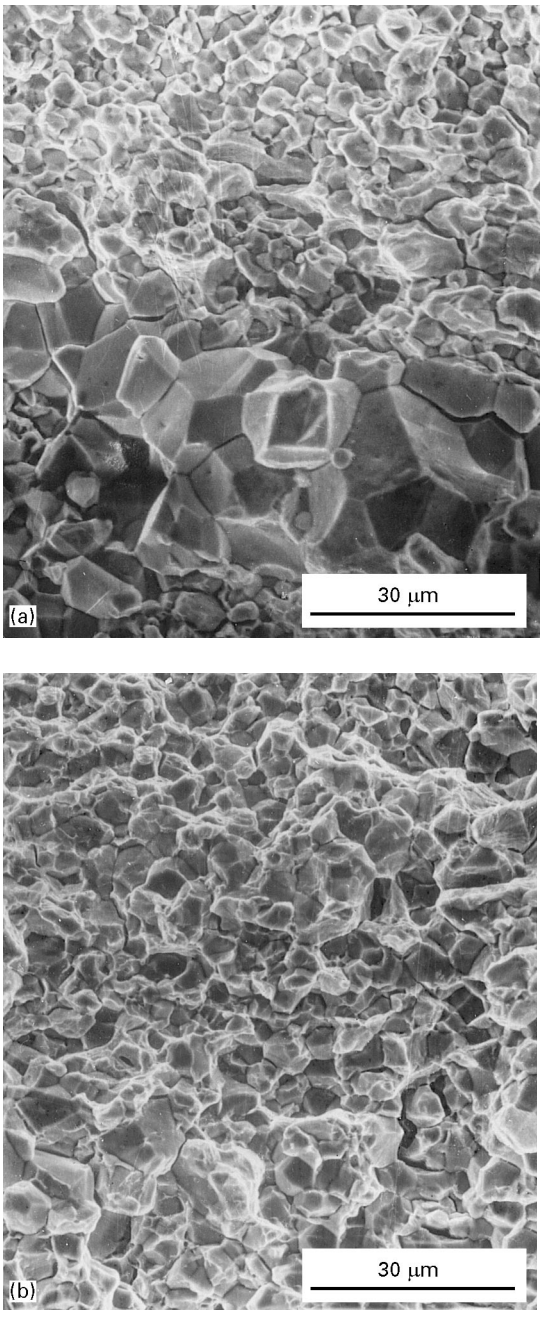

Figure 2 SEM fractographs of the alloy 1 samples isothermally treated at (a) 750 °C and (b) 1000 °C.

of quasi-cleavage fracture (Fig. 3a) while those isothermally treated at either 750 or 1000 °C present complete ductile fracture (Fig. 3b). The above results on fractography are in good agreement with those from the tensile tests.

The following may be concluded from Figs 1–3 and Table II: (i) for alloy 1 containing cerium, the grain-boundary cohesion of the samples isothermally treated at 550 or 1200 °C is obviously enhanced, whereas that of the samples isothermally treated at 750 or 1000 °C is not; (ii) for alloy 2 containing boron and alloy 3 containing both cerium and boron, all the mechanical properties are comprehensively better than those for alloy 1; (iii) the results of the fractography are in agreement with those from the tensile tests.

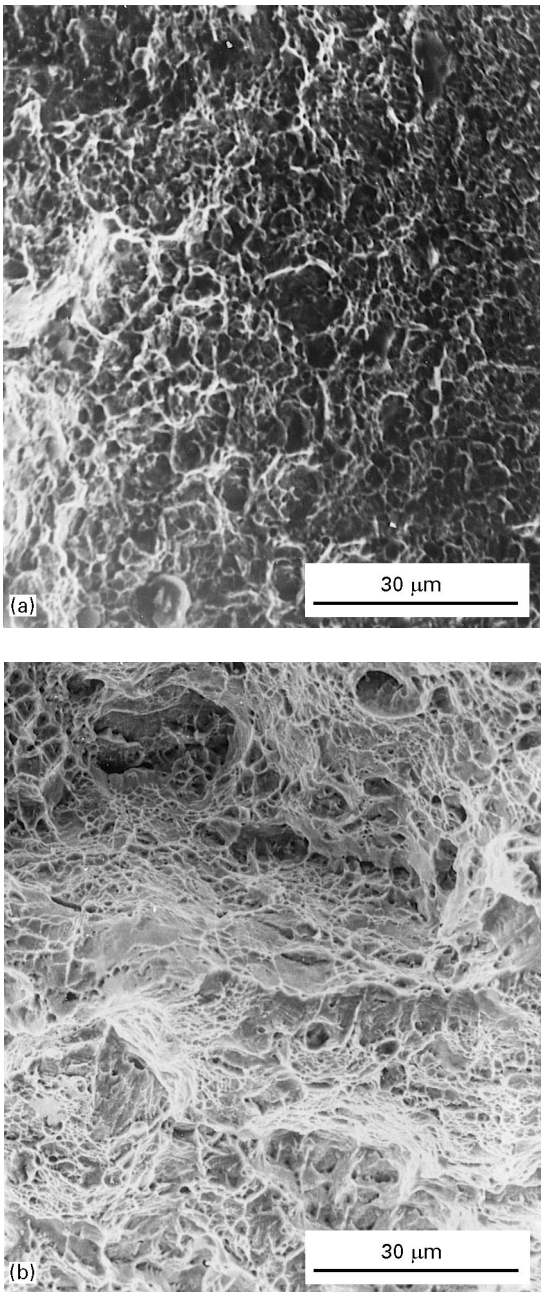

Figure 3 Typical SEM fractographs of the alloy 3 samples isothermally treated at (a) either 550 or 1200 °C and (b) either 750 or 1000 °C.

3.3. Microstructure

TEM for all the samples demonstrated that there was no apparent precipitation either along the grain boundaries or within the grains. Fig. 4 shows transmission electron micrographs of the samples from alloy 3 isothermally treated at different temperatures. Evidently there is no apparent precipitation at any isothermal-treatment temperature.

3.4. Oxidation behaviour

The mass increase of the sample that was oxidized for different times is illustrated in Figs 5 and 6 as a function of oxidation time. The thickness of oxidation layer increases with increasing oxidation time or temperature. For 1000 °C oxidation (see Fig. 5), the mass increase of alloy 1 is slightly less than that of alloy 2; nevertheless, it is much larger than that of alloy 3. For 1100 °C oxidation (see Fig. 6), the mass increase rises obviously on going from alloy 3 to alloy 1 to alloy 2 at the same oxidation time. In summary, alloy 3 containing both cerium and boron, of the three alloys concerned, has the best isothermal oxidation resistance, and alloy 1 containing cerium exhibits a better oxidation resistance than alloy 2 containing boron.

4. Discussion

4.1. Tensile properties

It is well known that intergranular fracture of polycrystalline Ni_3Al occurs easily because of poor grain-boundary cohesion. The results presented in this work indicate that minor additions of cerium to this aluminide, under some conditions, improve its ductility. However, the improvement in ductility of Ce-doped Ni_3Al is strongly dependent on the total quantity of cerium added and its distribution. If the cerium addition in Ni_3Al is higher, a second phase containing cerium may be able to precipitate along the grain boundary so as to cause the ductility of the alloy to deteriorate. It has been demonstrated [12] that the appropriate amount of cerium addition in Ni_3Al appears to be between 0.0083 and 0.044 wt %.

In addition, the present results also show that the alloy doped with boron or with both cerium and boron exhibits good mechanical properties compared with that doped with cerium for all the heat-treatment conditions adopted and that the mechanical properties for the alloy doped with both cerium and boron are comprehensively better than those for the alloy doped with boron. This suggests that the combined effects of cerium and boron additions should be applicable to modifying a Ni_3Al alloy.

The effects of cerium and boron on grain-boundary cohesion in Ni_3Al may be explained by the following electronic model [15, 16]. Both cerium and boron are of lower electronegativity than the base metals (Ni, Fe, etc.). These elements do not draw charge off the base metal atoms and thus do not weaken the base metal–base metal bonds. Moreover, cerium is a metal element and its metallic nature is very strong. Thus, cerium atoms and base metal atoms together form metal–metal bonds and share electrons. Apart from

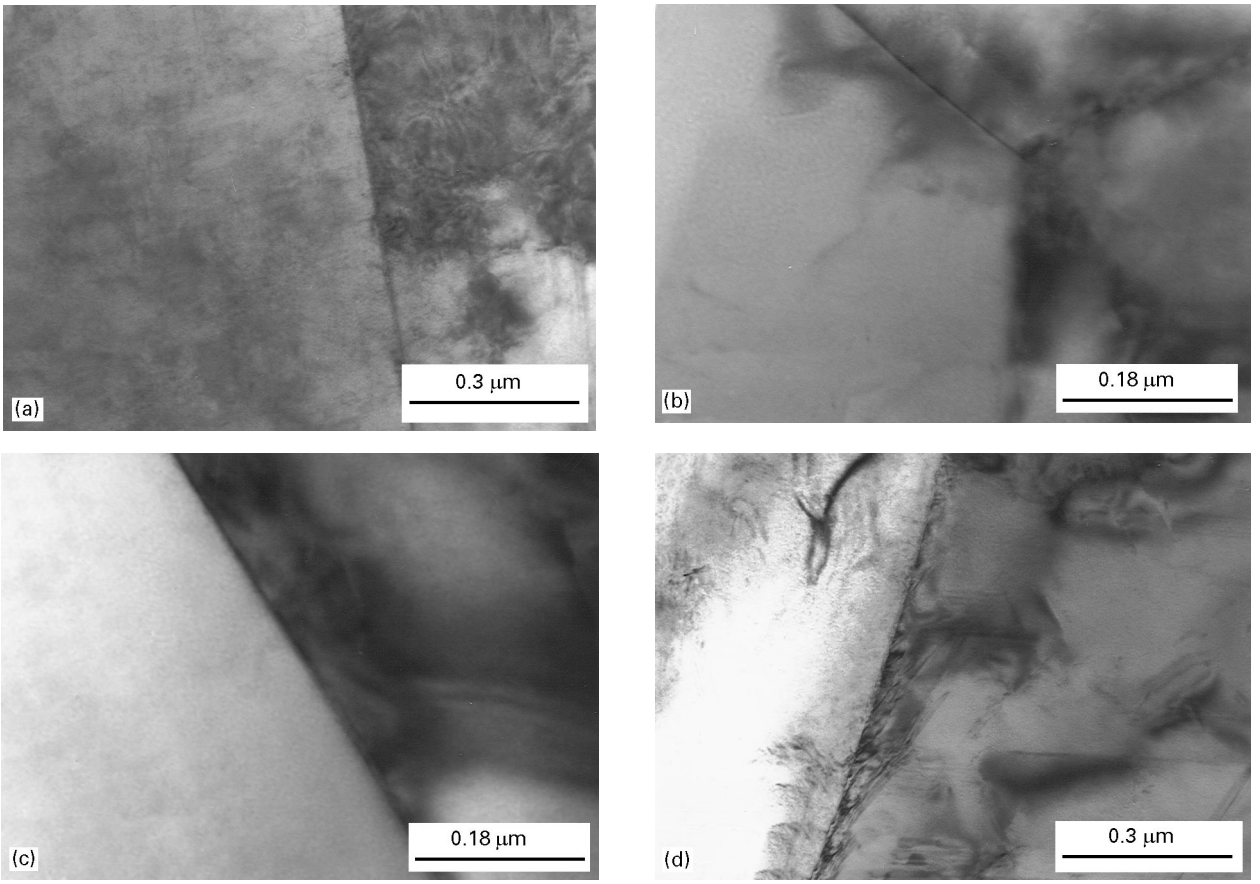

Figure 4 Transmission electron micrographs of the alloy 3 samples isothermally treated at (a) 550 °C, (b) 750 °C, (c) 1000 °C and (d) 1200 °C.

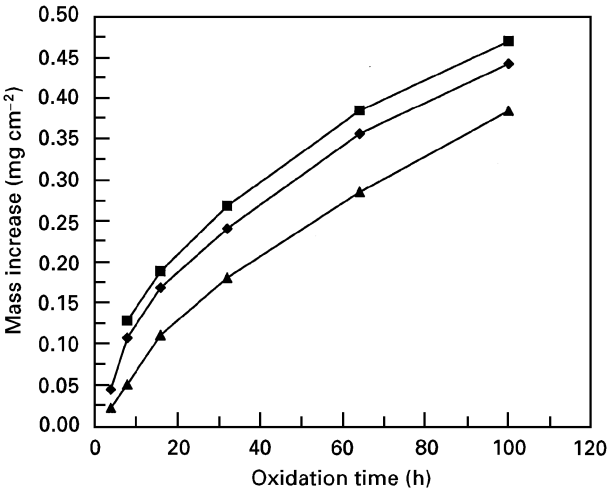

Figure 5 Mass increases of the sample after they had been oxidized for different times at 1000 °C. (–◆–), alloy 1; (–■–), alloy 2; (–▲–), alloy 3.

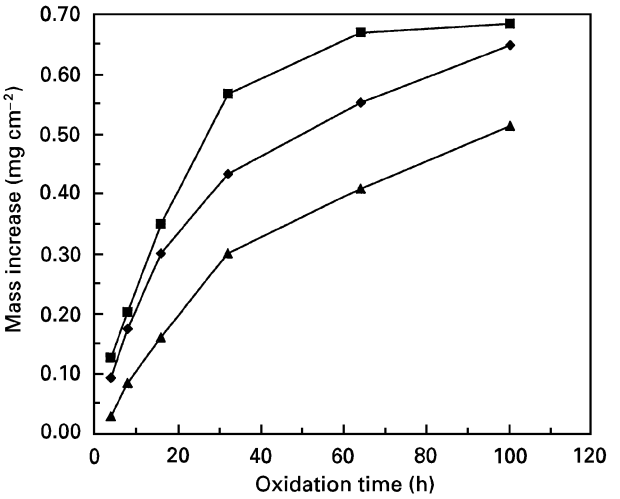

Figure 6 Mass increases of the sample after they had been oxidized for different times at 1100 °C. (–◆–), alloy 1; (–■–), alloy 2; (–▲–), alloy 3.

the above, a pair bonding theory [17] suggests that the segregation of boron can result in an increase in grain-boundary fracture energy. Therefore, cerium and boron are beneficial elements for improvement in the grain-boundary cohesion. In addition, cerium has a strong affinity with sulfur and its effect may result from the scavenging of sulfur from grain boundaries.

For the above reasons, cerium and boron, which tend to segregate strongly at the grain boundary in Ni_3Al [6, 18, 19], may be able to enhance bonding in the grain boundary, which results in an improvement in grain-boundary cohesion and a reduction in the trend to brittle intergranular fracture. Considerable grain-boundary segregation of boron without boride precipitation in the 0.07 wt % B-doped Ni_3Al alloy samples isothermally treated at temperatures similar to those used in this work and then water quenched has been confirmed in [19]. However, if the

segregation level of cerium at the grain boundary is too high, the precipitation of a second phase containing cerium will be able to take place along the grain boundary, resulting in intergranular fracture of the alloy; if the segregation level is too low, the grain-boundary cohesion will also not be improved. It has been shown in this work that no apparent grain-boundary precipitation emerges in any isothermally treated sample. Therefore, it may be thought that the cerium segregation level in the samples isothermally treated at either 750 or 1000 °C is probably not high enough to make the grain-boundary cohesion enhanced considerably; yet this may be remedied by boron segregation [11, 19].

The experimental results cannot be explained merely by an equilibrium segregation mechanism [20] because equilibrium segregation is a thermodynamic process and decreases with increasing annealing temperature. However, they may be reasonably interpreted with the aid of a combined equilibrium and non-equilibrium segregation mechanism [21]. Non-equilibrium segregation is a kinetic process and increases with increasing annealing temperature.

In order to use the combined equilibrium and non-equilibrium segregation mechanism to explain the experimental results, it is necessary to describe succinctly the non-equilibrium segregation mechanism. The mechanism relies on the formation of sufficient quantities of vacancy–solute complexes. Solute atoms, vacancies and their complexes are in equilibrium with each other at a given temperature. When a material which is properly held at an annealing temperature is quickly cooled to a lower temperature, it will exhibit a loss of vacancies along grain boundaries, i.e., at vacancy sinks, whereby it achieves the equilibrium vacancy concentration corresponding to the lower temperature. The decrease in vacancy concentration brings about the dissociation of the complexes into vacancies and solute atoms. This in turn leads to a decrease in complex concentration in the neighbourhood of grain boundaries. Meanwhile, in regions remote from the grain boundary, where no other vacancy sinks are present, the vacancy concentration, which is nearly equal to the equilibrium vacancy concentration corresponding to the annealing temperature, always remains. As a result, a complex concentration gradient appears between the grain boundary and the adjacent grains. The concentration gradient of the complexes causes their migration, leading to an excess solute concentration in the vicinity of grain boundaries. It is obvious that, the larger the supersaturation level of vacancies induced by the heat treatment, the larger is the segregation level of solute atoms resulting at the boundary.

In the light of the combined segregation mechanism, the experimental results may be explained as follows. For the samples treated at 750 and 1000 °C, the segregation of cerium arises from combined equilibrium and non-equilibrium segregation, but the segregation level is not high enough to improve the ductility of the alloy whereas it is for the samples treated at 550 and 1200 °C. In the 550 °C-treated sample, most of the segregation is caused by the equilibrium segregation mechanism, but in the 1200 °C-treated sample it is caused mainly by the non-equilibrium segregation mechanism.

4.2. Oxidation behaviour

The present oxidation examination demonstrates that alloy 3 doped with both cerium and boron, of the three alloys concerned, exhibits the best oxidation resistance, and alloy 1 doped with cerium shows a better oxidation resistance than alloy 2 doped with boron does.

As stated in the introduction section, the oxidation resistance of Ni_3Al depends on the formation of dense Al_2O_3 film at its surface. Optical microscopy of the cross-sections of the oxidized samples may be summarized as follows. The outer layer consists of oxidation scales, which have spalled off mostly during cooling. At the same oxidation temperature, the scale that spalled off during cooling decreases on going from alloy 2 to alloy 1 to alloy 3. Between the outer layer and the Ni_3Al matrix is γ-solid solution, which is produced by diffusion of aluminium atoms to the outer oxidation layer. In general, the extent of the γ-solid solution increases with increasing oxidation temperature or time. X-ray diffraction analysis for both the oxidation layer and the scale spalling off during cooling may be summarized as follows. For alloy 1 and alloy 2, the outer part of the oxidation layer, after oxidation for 100 h, is NiO, and the inner part Al_2O_3, and there appears to be no cerium oxide or boron oxide. For alloy 3, however, the oxidation layer at the same oxidation condition is mostly Al_2O_3 with a very small amount of Al_3BO_6 and $CeAlO_3$. The scale spalling off during cooling is just $NiAl_2O_4$, which is induced by a chemical reaction between NiO and Al_2O_3 at high temperatures.

Cerium and boron both are active with respect to the surfaces and tend to segregate to them. Surface segregation of cerium and boron may lead to a considerable reduction in the surface diffusion coefficient of nickel atoms [22]. The reduction in the nickel diffusion coefficient is beneficial to restraining the formation of NiO film that has a low capability of protecting the surface from being oxidized further, which in turn makes the chemical reaction between NiO and Al_2O_3 difficult and causes the highly protective Al_2O_3 to exist stably [23, 24].

Electron probe analysis for cerium-doped Fe–Cr–Al alloys oxidized at a high temperature [24] demonstrates that only Al and O instead of Fe and Cr exist in the oxidation layer, which implies that cerium may promote the preferential oxidation of aluminium. Consequently, alloy 1 doped with cerium exhibits a better oxidation resistance than alloy 2 doped with boron. However, reasons why alloy 3 doped with both cerium and boron, of the three alloys concerned, presents the best oxidation resistance require to be sought further.

5. Conclusions

1. The ductility of Ce-doped Ni_3Al alloy strongly depends on the cerium distribution. When 0.011 wt %

Ce-doped Ni_3Al alloy is isothermally treated at 550 °C for 120 h or at 1200 °C for 0.5 h, the tensile elongation and ultimate strength at room temperature may reach about 16% and about 900 MPa, respectively, and the alloy exhibits almost completely transgranular fracture. When the alloy is isothermally treated at 750 °C for 40 h or at 1000 °C for 1 h, the tensile elongation and ultimate tensile strength are only about 3% and about 500 MPa, respectively, and the alloy exhibits brittle intergranular fracture.

2. Both alloy 2 (containing boron) and alloy 3 (containing both cerium and boron) exhibit good yield and ultimate strengths compared with alloy 1 (containing cerium). However, the yield strength of alloy 3 is much higher than that of alloy 2; alloys 2 and 3 both present much greater elongation than alloy 1; nevertheless, the elongation of alloy 2 is somewhat higher than that of alloy 3. Consequently alloy 3 has comprehensively the best mechanical properties of the three alloys concerned.

3. Alloy 3 exhibits, of the three alloys concerned, the best oxidation resistance. Alloy 1 presents a better oxidation resistance than alloy 2 does.

Acknowledgement

This work was supported by the Science and Technology Division of the Metallurgical Ministry of China.

References

1. J. H. WESTBROOK and R. L. FLEISCHER (eds), "Intermetallic compounds", Vol. 1 (Wiley, Chichester, West Sussex, 1995) pp. 977–1016.
2. *Idem*., *ibid*. Vol. 2 (Wiley, Chichester, West Sussex, 1995) pp. 3–52.
3. T. TAKASUGI and O. IZUMI, *Acta Metall.* **33** (1985) 1247.
4. T. TAKASUGI, O. IZUMI and N. MASAHASHI, *ibid.* **33** (1985) 1259.
5. T. TAKASUGI, E. P. GEORGE, D. P. POPE and O. IZUMI, *Scripta Metall.* **19** (1985) 551.
6. C. T. LIU, C. L. WHITE and J. A. HORTON, *Acta Metall.* **33** (1985) 213.
7. C. T. LIU, *Scripta Metall. Mater.* **27** (1992) 25.
8. E. P. GEORGE, C. T. LIU and D. P. POPE, *ibid.* **28** (1993) 857.
9. J.-S. WANG, *Mater. Sci. Engng* **A192–A193** (1995) 371.
10. K. AOKI and O. IZUMI, *J. Japan Inst. Metals* **43** (1979) 1190.
11. S.-H. SONG, Z.-X. YUAN, T.-D. XU and Z.-S. YU, *Scripta Metall. Mater.* **24** (1990) 1857.
12. Z.-X. YUAN, S.-H. SONG, T.-H. XI, X.-J. ZHANG and Z.-S. YU, *J. Mater. Sci. Lett.* **13** (1994) 1717.
13. J. GUO, C. SUN, H. LI and H. GUAN, *Acta Metall. Sin.* (*Engl. Edn*) *B* **3** (1990) 38.
14. M. J. SEAVERS and J. E. WHITTLE, *Sheet Metal Ind.* **51** (1974) 250.
15. C. L. BRIANT and R. P. MESSMER, *Phil. Mag. B* **12** (1980) 569.
16. R. P. MESSMER and C. L. BRIANT, *Acta Metall.* **30** (1982) 457.
17. M. P. SEAH, *ibid.* **28** (1980) 955.
18. S.-H. SONG, T.-D. XU, Z.-X. YUAN and Z.-S. YU, *Scripta Metall.* **23** (1989) 1291.
19. D.-L. LIN, D. CHEN and H. LIN, *Acta Metall. Mater.* **39** (1991) 523.
20. D. McLEAN, "Grain boundaries in metals" (Oxford University Press, London, 1957) p. 118.
21. S.-H. SONG and T.-D. XU, *J. Mater. Sci.* **29** (1994) 61.
22. T. C. CHOU and Y. T. CHOU, *Mater. Res. Soc. Symp. Proc.* **39** (1985) 461.
23. S. TANIGUCHI, T. SHIBATA and H. TSURUOKA, *Oxid. Met.* **26** (1986) 1.
24. YU ZONGSEN, "Rare-earths in steels" (Metallurgical Industry Press, Beijing, 1984) p. 196.

Received 21 May 1996
and accepted 20 August 1997